 CMES, vol.53, no.3, pp.303-325, 2009

Cusp-Catastrophe Interpretation of the Stick-Slip Behaviour of Rough Surfaces

A. Carpinteri[1], M. Paggi[1,2] and G. Zavarise[3]

Abstract: The stick-slip instability is a typical manifestation of the nonlinearity of the frictional response of rough surfaces. As recently demonstrated by several researchers, the problem of contact loss is also inherently connected to the stick-slip instability and it has been detected both in elastically soft materials, such as rubber or gelatine, and in elastic stiff materials, such as for earthquake faults. Treating the problem of tangential contact in the framework of micromechanical contact models, the effect of the phenomenon of contact loss on the micro-slip behavior of rough surfaces is herein investigated. To this aim, the stick and slip components of the total applied tangential force and of the total real contact area are properly determined as functions of the total applied tangential force. A comparison with the behavior of smooth surfaces, such as spheres, cylinders and flat surfaces, is presented. Then, simulating the problem of tangential loading followed by a reduction of the applied normal force, it will be shown that the phenomenon of contact loss gives rise to energy release due to snap-back instability in the diagram relating the tangential force to the sliding displacement. This result provides for the very first time an explanation to the phenomenon of stick-slip according to the Catastrophe Theory, in close analogy with the cusp-catastrophe instability of Mode I crack propagation in cohesive solids.

Keywords: Contact Mechanics, rough surfaces, mechanical instability, stick-slip, contact loss.

1 Introduction

The problem of contact between two solids with rough boundaries is a complex nonlinear phenomenon where the multiscale properties of rough surfaces play a fundamental role (Persson, 2001; Borri-Brunetto et al., 2006a; Nosonovsky and

[1] Politecnico di Torino, Department of Structural and Geotechnical Engineering, Torino, Italy
[2] Corresponding author, email: marco.paggi@polito.it
[3] University of Salento, Department of Innovation Engineering, Lecce, Italy

Bhushan, 2007; Yao and Gao, 2007; Ciavarella et al., 2008; Sainsot et al., 2002; Willner, 2009; Chen and Atkinson, 2009; Galli and Oyen, 2009; García-Aznar, Pérez and Moreo, 2009). As an example regarding the normal contact problem, the surface waviness makes unstable the detachment process of an elastic half-space from a rigid solid in the presence of adhesion, as recently demonstrated in (Guduru, 2007; Guduru and Bull, 2007).

As far as the tangential contact problem is concerned, a fundamental evidence of nonlinearity and discontinuity in the tangential contact behaviour is represented by the so-called phenomenon of stick-slip (Kikuchi and Oden, 1988; Song et al. 2005). Since the static friction force is greater than the kinetic friction force, in a situation when a steadily increasing tangential force is applied to a body, sticking of two bodies results into a steadily increase of the applied force. When the applied force exceeds the static friction, the resistance instantaneously drops to the value of the kinetic friction. This results into a decrease in the applied shear force and a deceleration until the body sticks again, giving rise to an alternation of stick and slip phases. From the experimental point of view, the typical frictional forces observed in the different dynamical regimes are shown in Fig. 1. For lower sliding velocities, the stick-slip motion can be clearly observed, whereas such an instability disappears for higher sliding velocities and reverts to smooth sliding. For elastically soft materials such as rubber, elastic instabilities responsible for the stick-slip motion are the so-called Schallamach waves (Persson, 2001). At a high enough sliding velocity, the rubber surface in front of an asperity undergoes a buckling that gives rise to detachment waves, propagating like wrinkles in a carpet. Using a state-and-rate dependent friction law and performing a linear stability analysis, Persson (2001) proved that the Schallamach waves can be considered as a stress relieving mechanism limiting the buildup of friction with speed. It is interesting to note that the interfacial stick-slip phenomenon can also occur in elastically stiffer materials, such as for earthquake faults, where again a state-and-rate dependent friction law can be adopted for the study of their chaotic response (Putelat et al, 2007). In such large-scale systems, the experimental evidence of the phenomenon of contact loss, already observed by Persson (2001) on a smaller scale connected to the propagation of the Schallamach wawes, was recently obtained by Bouissou et al. (1998). In their tests, a shear load was transmitted to two rough surfaces by a testing machine which imposed a global relative movement at a constant sliding velocity. Under these conditions, energy dissipations take place, like during the stick-slip motion of a fault, and a relative opening displacement in the direction normal to the interface was experimentally measured.

The stick-slip instability seems therefore inherently connected to the phenomenon of contact loss, giving prominence to the pioneering investigations by Comninou

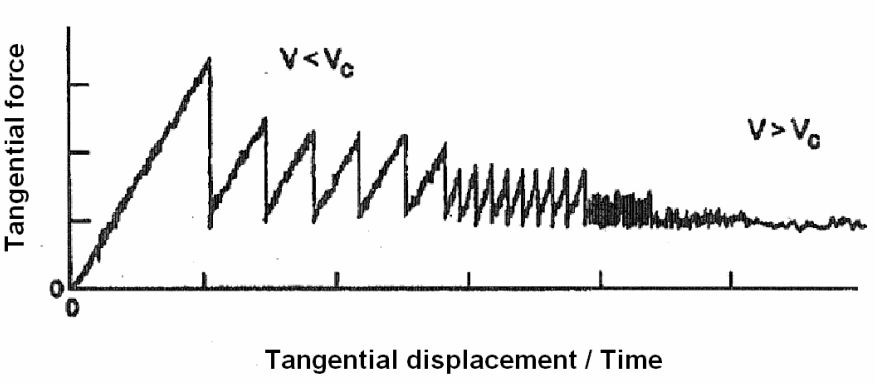

Figure 1: Typical stick-slip instability of a mechanical system (adapted from Yoshizawa et al. (1993)).

and Dundurs (1978). They theoretically demonstrated that, when two smooth elastic solids are pressed together and at the same time sheared, they can undergo a sliding motion without slip at the interface, due to the occurrence of contact loss, as occurs for the propagation of a carpet fold. A possible explanation of contact loss in rigid body systems was recently provided by Frémond and Isabella-Valenzi (2006). When a rigid body slides over a frictional surface, hopping motion is very often observed. The motion of rigid bodies in the presence of friction introduces reaction forces that depend on the vertical and sliding velocities through algebraic or differential equations. For certain kinematic and geometric conditions, it is possible to have infinite reaction forces. In such a situation, the smooth evolution is no longer possible and contact loss can take place. For instance, this is the case of the Painlevé sthenic incompatibility, observed when moving a piece of chalk on a blackboard (Frémond and Isabella-Valenzi, 2006).

In the present contribution, starting from the preliminary results by Paggi et al. (2007), the effect of a partial or complete contact loss on the tangential motion of elastic bodies is analyzed in the context of rough contact surfaces in the absence of adhesion effects. In this framework, frictional dissipation starts growing for shear forces lower than the nominal static threshold. In fact, when an increasing tangential force is applied, small relative displacements occur locally along the contacting surface (micro-slip), before sliding (also referred to as full-slip) takes place. Micro-slip regime is important in different fields and also presents a fundamental interest related to the understanding of the microscopic mechanisms responsible for the observed size-scale effects on the macroscopic friction (Carpinteri and Paggi, 2005; Carpinteri and Paggi, 2008). So far, most of the research focused

on the energy dissipation occurring when two bodies are subjected to a constant normal force and an oscillating shear force (Kirsonava, 1967; Desai et al., 1985; Rooke and Edwards, 1988; Harnoy et al., 1994). From the mathematical point of view, this problem was firstly addressed by Mindlin and Deresiewicz (1953), according to the well-known Cattaneo-Mindlin's analogy (Cattaneo, 1938; Mindlin, 1949). They investigated the frictional phenomena occurring at the contact surfaces of elastic spheres subjected to a variety of applied forces. These theoretical predictions were also experimentally confirmed by Goodman and Brown (1962). More recently, Ciavarella (1998) and, independently, Jäger (1998) extended the validity of the Cattaneo-Mindlin's analogy, originally conceived for smooth contact surfaces, to the more applicative case of rough surfaces. Following this approach, a generalization of the Mindlin and Deresiewicz approach for cyclic loading was also recently proposed by Borri-Brunetto et al. (2006b).

Considering the problem of tangential contact with a quasi-static increase of the applied tangential force from zero up to a maximum value below the limit of full-sliding, we propose an analytical approach based on the Greenwood and Williamson contact model (Greenwood and Williamson, 1966) (see also Zavarise et al. (2004); Zavarise et al. (2007) for a detailed description of the micromechanical model, its input parameters and outcomes). This micromechanical model, originally developed for the analysis of the normal contact problem, is herein applied to the analysis of contact in the tangential direction. A spherical shape for the contacting asperities is assumed, consistently with the hypotheses of the original Greenwood and Williamson model, and also put forward by Bureau et al. (2003). In our treatment, we focus the attention on the evaluation of the stick and slip components of the applied tangential force and the corresponding stick and slip portions of the real contact area. The closed-form solutions obtained using this model are presented in a useful non-dimensional form and are compared with the analogous results for smooth surfaces. To this end, the well-known solutions for the tangential contact of spheres, cylinders and ideal smooth planes reported in the fundamental book by Johnson (1985) are profitably extended to put into evidence the stick and slip components of the applied tangential force and of the contact area.

Finally, with these results in hand, we analyze the problem of tangential loading followed by a reduction in the applied normal force, simulating a partial or complete phenomenon of contact loss. As a main result, it will be shown that the phenomenon of contact loss can give rise to energy release due to snap-back instability in the tangential force vs. sliding displacement diagram. These results demonstrate that the stick-slip instability may also occur during the micro-slip motion of rough surfaces and manifests itself as a catastrophic snap-back instability, in close analogy with the unstable behavior of Mode I crack propagation in cohe-

sive solids (Carpinteri, 1989). The analysis proposed in the present work provides a mechanical interpretation of the instability responses found in the experimental tests where the relative tangential displacement of the blocks in contact is the control variable. This is for instance the case of the tests by Bouissou et al. (1998), where the applied relative tangential displacement is a steadily increasing function of time. On the other hand, if one is interested in the problem of sliding of a block over a rough surface with given prescribed initial conditions (for instance the sliding velocity), then the dynamic behaviour of the system has to be explicitly taken into account. This can be done by solving the equation of motion of the mechanical system considering its actual mass, stiffness, as well as the nonlinear relationship between tangential force and relative tangential displacement as in this work. Of course, these properties may depend on the specific mechanical application being considered.

2 Tangential contact of elastic rough surfaces

Let us consider the problem of normal contact between two rough surfaces having an identical r.m.s. roughness, σ, elastic modulus, E, and Poisson's ratio, ν. Taking advantage of the concept of *composite topography* introduced by Brown and Scholz (1985), we shall consider, without any loss of generality, the problem of contact between a composite rough surface and a rigid, ideally flat, reference plane. The composite topography is obtained by computing the difference between the maximum gaps and the current gaps of two corresponding points in the undeformed condition. This problem is mathematically analogous to the original one, provided that we use in the computations an equivalent r.m.s. roughness, $\sigma^* = \sqrt{2}\sigma$, an equivalent radius of curvature of the asperity tips, $\rho^* = \rho/\sqrt{2}$, and an effective elastic modulus of the composite surface $E^* = E/[2(1-\nu^2)]$.

We also consider, in the framework of the Greenwood and Williamson's micromechanical contact model (Greenwood and Williamson, 1966), rough surfaces whose summit heights follow a given statistical distribution, $\Phi(z)$, which is usually the Gaussian or the exponential one. The expressions of the derived equations are reported in the sequel for a general statistical distribution. In this general case, however, the required integrations have to be performed numerically. To obtain useful closed-form solutions, the formulae are also particularized to the special case of the exponential distribution

$$\Phi(z) = \frac{1}{\sigma^*} \exp\left(-\frac{z}{\sigma^*}\right) \tag{1}$$

where z is the summit height measured perpendicular to the mean plane of the rough surface (see Fig. 2).

For a given applied normal force, let us denote by d the distance between the mean plane of the rough surface and the reference plane (see Fig. 2). Therefore, each asperity in contact of height $z > d$ will experience a closure equal to $g_{\mathrm{N},i} = z - d$.

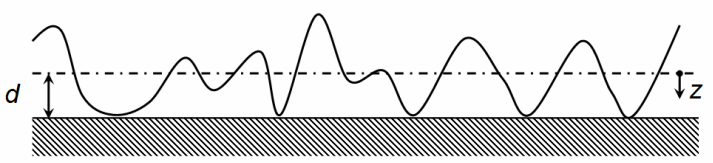

Figure 2: Contact between a composite rough surface and a smooth rigid plane.

When the remote (relative to distant points in the undeformed region of each body) tangential displacement, g_{T}, is progressively increased during the loading process, from zero up to a maximum value, say $g_{\mathrm{T}}^{\max}$, it is possible to determine the interface response under the assumption of spherical capped asperities. Thus, we can combine the well-known Hertz formulae for the normal contact with the relationship between the tangential displacement, g_{T}, and the applied shear force, F_{T} (Johnson, 1985)

$$g_{\mathrm{T}} = \frac{3\,(2-\nu)\,\mu g_{\mathrm{N}}}{8Ga}\left[1-\left(1-\frac{F_{\mathrm{T}}}{\mu F_{\mathrm{N}}}\right)^{2/3}\right] \tag{2}$$

where G is the shear modulus, ν the Poisson's ratio, a is the Hertz contact radius, F_{N} is the normal load and μ is the friction coefficient.

More specifically, the Hertz contact radius for the i-th microcontact, a_i, and the corresponding normal force, $F_{\mathrm{N},i}$, can be computed as functions of the normal gap, $g_{\mathrm{N},i} = z - d$, as follows

$$a_i = \sqrt{\rho^*\,(z-d)} \tag{3a}$$

$$F_{\mathrm{N},i} = \frac{4}{3}\frac{E^*}{\rho^*}a_i^3 = \frac{2}{3}\frac{E}{(1-\nu^2)}\sqrt{\rho^*}\,(z-d)^{3/2} \tag{3b}$$

Introducing these expressions into Eq. (2), and using $G = E/\left[2\,(1+\nu)\right]$, we obtain

$$\left(1-\frac{F_{\mathrm{T},i}}{\mu F_{\mathrm{N},i}}\right)^{2/3} = 1-\frac{g_{\mathrm{T}}\sigma^*}{\mu\lambda\,(z-d)} \tag{4}$$

where the symbol $\lambda = \sigma^*\,(2-\nu)\,/\,[2\,(1-\nu)]$ has been introduced to shorten notation. It is important to observe that the right hand side of Eq. (4) is positive, i.e. it

expresses a stick state, if and only if the following inequality holds

$$g_{\mathrm{N},i} = z - d \geq \frac{g_{\mathrm{T}}\sigma^*}{\mu\lambda} = g_{\mathrm{N},0} \tag{5}$$

Therefore, microcontacts whose closure is such that $g_{\mathrm{N},i} > g_{\mathrm{N},0}$ would support a stick tangential force $F_{\mathrm{T},i} \leq \mu F_{\mathrm{N},i}$. On the other hand, microcontacts having $g_{\mathrm{N},i} \leq g_{\mathrm{N},0}$ are sliding, i.e. $F_{\mathrm{T},i} = \mu F_{\mathrm{N},i}$. Hence, for the microcontacts having $g_{\mathrm{N},i} > g_{\mathrm{N},0}$, Eq. (4) combined with Eq. (3b) leads to the stick force

$$F_{\mathrm{T,i}} = \mu \frac{2E}{3\left(1-\nu^2\right)} \sqrt{\rho^*} (z-d)^{3/2} \left[1 - \left(1 - \frac{g_{\mathrm{T}}\sigma^*}{\mu\lambda\,(z-d)} \right)^{3/2} \right] \tag{6}$$

Therefore, the total tangential force supported by a unit area of the contact domain in stick condition, $F_{\mathrm{T}}^{\mathrm{ST}}$, can be obtained by integration over the height distribution

$$F_{\mathrm{T}}^{\mathrm{ST}} = \mu \frac{2E}{3\left(1-\nu^2\right)} \sqrt{\rho^*} n_s A_n \int_{d_0}^{\infty} \left[(z-d)^{3/2} - \left(z - d - \frac{g_{\mathrm{T}}\sigma^*}{\mu\lambda} \right)^{3/2} \right] \Phi(z)\, \mathrm{d}z \tag{7}$$

where the parameter d_0 is given by the condition (5), i.e. $d_0 = d + g_{\mathrm{N},0}$.

On the other hand, the total tangential force applied to the system is given by the sum of the stick and the slip, $F_{\mathrm{T}}^{\mathrm{SL}}$, ones

$$F_{\mathrm{T}} = F_{\mathrm{T}}^{\mathrm{ST}} + F_{\mathrm{T}}^{\mathrm{SL}} = \mu \frac{2E}{3\left(1-\nu^2\right)} \sqrt{\rho^*} n_s A_n \left\{ \int_{d_0}^{\infty} \left[(z-d)^{3/2} - \left(z - d - \frac{g_{\mathrm{T}}\sigma^*}{\mu\lambda} \right)^{3/2} \right] \Phi(z)\, \mathrm{d}z + \int_{d}^{d_0} (z-d)^{3/2} \Phi(z)\, \mathrm{d}z \right\} \tag{8}$$

where the second integral in braces corresponds to the contribution due to the contact domain in slip condition, which is obtained from Eq. (3b) multiplied by the friction coefficient, i.e., $F_{\mathrm{T},i}^{\mathrm{SL}} = \mu F_{\mathrm{N},i}$. Integrating Eq. (8), we derive the following closed-form relationship between the total tangential force and the sliding displacement, provided that an exponential distribution of asperity heights, like the one given by Eq. (1), is considered

$$F_{\mathrm{T}} = \mu F_{\mathrm{N}} \left[1 - \exp\left(-\frac{g_{\mathrm{N},0}}{\sigma^*} \right) \right] = \mu F_{\mathrm{N}} \left[1 - \exp\left(-\frac{g_{\mathrm{T}}}{\mu\lambda} \right) \right] \tag{9}$$

Comparing Eqs. (7) and (8), it is possible to determine the following relationship between the stick component of the tangential force, $F_{\mathrm{T}}^{\mathrm{ST}}$, and the total tangential

force, F_{T}

$$F_{\mathrm{T}}^{\mathrm{ST}} = F_{\mathrm{T}} - F_{\mathrm{T}}^{\mathrm{SL}} = F_{\mathrm{T}} - \mu \frac{2E}{3\left(1-\nu^2\right)} \sqrt{\rho^*} n_s A_n \int_d^{d_0} (z-d)^{3/2} \Phi(z)\, \mathrm{d}z \tag{10}$$

Recalling that the total normal load on the interface is given by (Greenwood and Williamson, 1966)

$$F_{\mathrm{N}} = \frac{4}{3} E^* \sqrt{\rho^*} n_s A_n \int_d^{\infty} (z-d)^{3/2} \Phi(z)\, \mathrm{d}z \tag{11}$$

it is possible to recast the relationship between $F_{\mathrm{T}}^{\mathrm{ST}}$and F_{T} in a nondimensional form. For the case of an exponential distribution of the asperity heights, from Eqs. (10) and (11) we have

$$\widehat{F}_{\mathrm{T}}^{\mathrm{ST}} = \frac{F_{\mathrm{T}}^{\mathrm{ST}}}{\mu F_{\mathrm{N}}} = \frac{F_{\mathrm{T}}}{\mu F_{\mathrm{N}}} - \frac{\int_d^{d_0} (z-d)^{3/2} \Phi(z)\, \mathrm{d}z}{\int_d^{\infty} (z-d)^{3/2} \Phi(z)\, \mathrm{d}z} = \widehat{F}_{\mathrm{T}} - \frac{\int_d^{d_0} (z-d)^{3/2} \Phi(z)\, \mathrm{d}z}{\int_d^{\infty} (z-d)^{3/2} \Phi(z)\, \mathrm{d}z} =$$

$$= \widehat{F}_{\mathrm{T}} - \frac{\exp\left(-\frac{g_{\mathrm{T}}}{\mu\lambda}\right)}{3\sqrt{\pi}} \left[-4 \left(\frac{g_{\mathrm{T}}}{\mu\lambda}\right)^{3/2} - 6 \left(\frac{g_{\mathrm{T}}}{\mu\lambda}\right)^{1/2} \right] - \mathrm{erf}\left[\left(\frac{g_{\mathrm{T}}}{\mu\lambda}\right)^{1/2} \right] =$$

$$= \widehat{F}_{\mathrm{T}} - \frac{1-\widehat{F}_{\mathrm{T}}}{3\sqrt{\pi}} \left\{ -4 \left[\sqrt{-\ln\left(1-\widehat{F}_{\mathrm{T}}\right)} \right]^3 - 6\sqrt{-\ln\left(1-\widehat{F}_{\mathrm{T}}\right)} \right\} -$$

$$- \mathrm{erf}\left[\sqrt{-\ln\left(1-\widehat{F}_{\mathrm{T}}\right)} \right] \Bigg\} \tag{12}$$

where the nondimensional terms $\widehat{F}_{\mathrm{T}} = F_{\mathrm{T}}/\mu F_{\mathrm{N}}$ and $\widehat{F}_{\mathrm{T}}^{\mathrm{ST}} = F_{\mathrm{T}}^{\mathrm{ST}}/\mu F_{\mathrm{N}}$ have been introduced, together with the relationship between $g_{\mathrm{T}}/\mu\lambda$ and $\widehat{F}_{\mathrm{T}}$ given in Eq. (9).

Similarly, the real contact area is given by the following formula (Greenwood and Williamson, 1966)

$$A_{\mathrm{r}} = \pi \rho^* n_s A_n \int_d^{\infty} (z-d) \Phi(z)\, \mathrm{d}z \tag{13}$$

and its part in stick condition can now be determined as

$$A^{\mathrm{ST}} = A_{\mathrm{r}} - \pi \rho^* n_s A_n \int_d^{d_0} (z-d) \Phi(z)\, \mathrm{d}z \tag{14}$$

Hence, after some algebra, it is possible to establish a relationship between the nondimensional contact area in stick condition, $\widehat{A}^{\mathrm{ST}} = A^{\mathrm{ST}}/A_{\mathrm{r}}$, where A_{r} is the total real contact area, and the nondimensional applied tangential force, $\widehat{F}_{\mathrm{T}}$

$$\widehat{A}^{\mathrm{ST}} = \frac{A^{\mathrm{ST}}}{A_{\mathrm{r}}} = 1 - \frac{\int_{d}^{d_0} (z-d)\Phi(z)\,\mathrm{d}z}{\int_{d}^{\infty} (z-d)\Phi(z)\,\mathrm{d}z} = \\ = \exp\left(-\frac{g_{\mathrm{T}}}{\mu\lambda}\right)\left(1+\frac{g_{\mathrm{T}}}{\mu\lambda}\right) = \left(1-\widehat{F}_{\mathrm{T}}\right)\left[1-\ln\left(1-\widehat{F}_{\mathrm{T}}\right)\right] \quad (15)$$

where, again, the relationship between $g_{\mathrm{T}}/\mu\lambda$ and $\widehat{F}_{\mathrm{T}}$ given by Eq. (9) has been used.

3 Tangential contact of smooth surfaces

3.1 Spheres

Two identical spherical bodies pressed into contact by a normal force, F_{N}, develop a circular area of contact. Its radius, a, and the ellipsoidal pressure distribution are given by the Hertz theory. If a suitably applied tangential force $F_{\mathrm{T}} < \mu F_{\mathrm{N}}$ is successively applied in the x direction at the interface level (see Fig. 7.1 in Chapt. 7 of Johnson, 1985), causing elastic deformation without slip at the interface, then the tangential displacement of all the points in the contact area is the same. Correspondingly, the distribution of tangential tractions, $q_x(r)$, is radially symmetric in magnitude and everywhere parallel to the x-axis (see e.g. Mindlin and Deresiewicz, 1953; Johnson, 1985, pag. 216)

$$q_x(r) = \mu \frac{3F_{\mathrm{N}}}{2\pi a^2}\left[1-\left(\frac{r}{a}\right)^2\right]^{-1/2} \quad (16)$$

This tangential traction corresponding to full-stick condition rises to a theoretically infinite value at the periphery of the contact circle, so that micro-slip is inevitable at the edge of contact, i.e. for $r \to a$ (see Fig. 3).

The axial symmetry of the tangential tractions $q_x(r)$ suggests that the stick region might be circular and concentric with the contact circle, whereas an annulus of slip is expected to develop inwards from the periphery of the contact area. In the case of partial slip, the Cattaneo-Mindlin's technique (Cattaneo, 1938; Mindlin, 1949) can profitably be applied and shows that the traction distribution along the contact

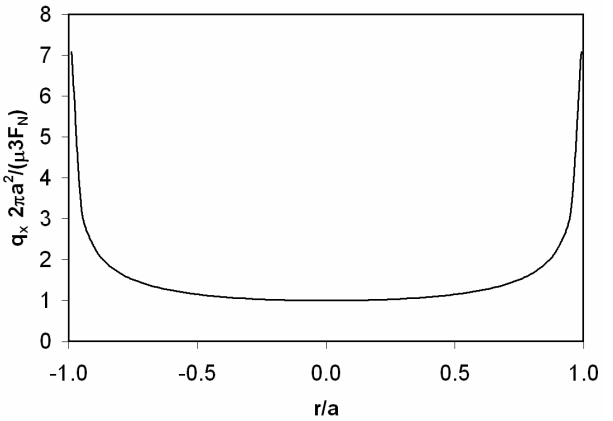

Figure 3: Distribution of tangential tractions for spheres in the case of full-stick condition.

area can be obtained by superposition of the following traction distributions

$$q_1(r) = \mu \frac{3F_{\mathrm{N}}}{2\pi a^2}\sqrt{1-\left(\frac{r}{a}\right)^2}, \quad 0 \le r \le a \tag{17a}$$

$$q_2(r) = -\mu \frac{3F_{\mathrm{N}}}{2\pi a^2}\frac{c}{a}\sqrt{1-\left(\frac{r}{c}\right)^2}, \quad 0 \le r \le c \tag{17b}$$

that are plotted in Fig. 4. The parameter c denotes the radius of the stick contact circle, whose value can be found from the condition of equivalence between the resultant of the traction distribution and the applied tangential force

$$F_{\mathrm{T}} = \int_0^a 2\pi q_1 r \, \mathrm{d}r + \int_0^c 2\pi q_2 r \, \mathrm{d}r = \mu F_{\mathrm{N}}\left[1-\left(\frac{c}{a}\right)^3\right] \tag{18}$$

whence:

$$\frac{c}{a} = \sqrt[3]{1-\frac{F_{\mathrm{T}}}{\mu F_{\mathrm{N}}}} = \sqrt[3]{1-\widehat{F}_{\mathrm{T}}} \tag{19}$$

Therefore, the resultant tangential traction acts parallel to the x-axis at all points and is given by $q_1(r)$ in the annulus $c \le r \le a$ and by $q_1(r)+q_2(r)$ in the central circle $0 \le r \le c$. It is also interesting to note that the applied tangential force can be decomposed into two parts: the former supported by the contact domain in stick

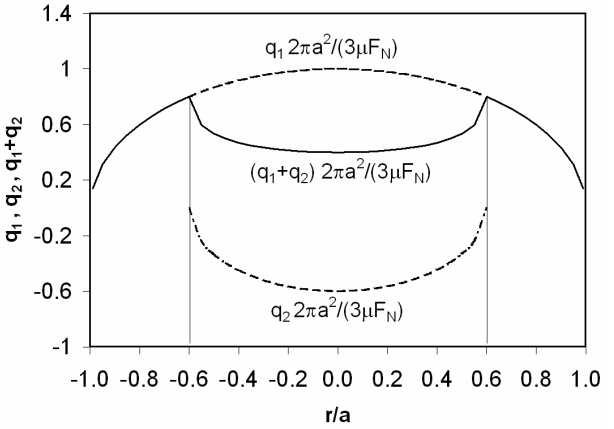

Figure 4: Traction distributions for spheres under partial slip conditions (c/a=0.6).

condition, $F_{\mathrm{T}}^{\mathrm{ST}}$, and the latter supported by the remaining part in slip condition, $F_{\mathrm{T}}^{\mathrm{SL}} = F_{\mathrm{T}} - F_{\mathrm{T}}^{\mathrm{ST}}$. As for rough surfaces, this decomposition is an original procedure and the derived formulae cannot be found elsewhere. Focusing our attention on the stick contribution, we can write

$$F_{\mathrm{T}}^{\mathrm{ST}} = \int_0^c 2\pi q_1 r \, \mathrm{d}r + \int_0^c 2\pi q_2 r \, \mathrm{d}r = \mu F_{\mathrm{N}} \left\{ 1 - \left[1 - \left(\frac{c}{a} \right)^2 \right]^{3/2} - \left(\frac{c}{a} \right)^3 \right\} \tag{20}$$

which can also be expressed as a function of the applied tangential force, using the relationship between c/a and $\widehat{F}_{\mathrm{T}}$ in Eq. (19)

$$\widehat{F}_{\mathrm{T}}^{\mathrm{ST}} = \widehat{F}_{\mathrm{T}} - \left[1 - \left(1 - \widehat{F}_{\mathrm{T}} \right)^{2/3} \right]^{3/2} \tag{21}$$

where the previously defined nondimensional variables $\widehat{F}_{\mathrm{T}}$ and $\widehat{F}_{\mathrm{T}}^{\mathrm{ST}}$ have been used. Finally, it is possible to establish a relationship between the nondimensional contact area in stick condition, $\widehat{A}^{\mathrm{ST}}$, and the nondimensional applied tangential force, $\widehat{F}_{\mathrm{T}}$

$$\widehat{A}^{\mathrm{ST}} = \frac{\pi c^2}{\pi a^2} = \left(\frac{c}{a} \right)^2 = \left(1 - \widehat{F}_{\mathrm{T}} \right)^{2/3} \tag{22}$$

where again we have introduced the relationship between c/a and $\widehat{F}_{\mathrm{T}}$.

3.2 Cylinders

Let us consider two identical and parallel cylinders in contact and pressed by a normal force per unit length, F_N. Both the contact line and their axes are parallel to the y-axis. A tangential force $F_T < \mu F_N$ per unit length is subsequently applied at the interface level (see Fig. 7.1 in Chapt. 7 of Johnson, 1985). Also in this case, the contact area represented by the contact strip of extension $2a$ and the pressure distribution are given by the Hertz theory. In full-stick condition, the distribution of tangential tractions is everywhere parallel to the x-axis and is given by (Johnson, 1985, pag. 214)

$$q(x) = \frac{F_T}{\pi a}\left[1-\left(\frac{x}{a}\right)^2\right]^{-1/2} \tag{23}$$

This tangential traction corresponding to full-stick condition rises to a theoretically infinite value at the edge of the contact strip, so that micro-slip is inevitable at the edge of contact, i.e. for $x \to \pm a$. Note that this traction distribution has the same trend as that for spheres (see Eq. (15)), provided that the variable r is substituted with x.

From the physical point of view, these high tangential tractions at the edge of the contact area cannot be sustained, since it would be required an infinite value of the friction coefficient. Therefore, micro-slip should take place starting from the edges of the contact strip. On the other hand, a stick region is expected in the centre of the strip where the tangential traction is lower and the normal pressure is higher. Applying again the Cattaneo-Mindlin's technique (Cattaneo, 1938; Mindlin, 1949), the traction distribution along the contact area in partial slip condition can be obtained by superposition of the following traction distributions:

$$q_1(x) = \mu\frac{2F_N}{\pi a}\sqrt{1-\left(\frac{x}{a}\right)^2}, \quad -a \le x \le a \tag{24a}$$

$$q_2(x) = -\mu\frac{2F_N}{\pi a}\frac{c}{a}\sqrt{1-\left(\frac{x}{c}\right)^2}, \quad -c \le x \le c,\ (c<a) \tag{24b}$$

where, in this case, c denotes one half of the width of the strip in stick condition, whose value can be found from the condition of equivalence between the resultant of the traction distribution and the applied tangential force

$$F_T = \int_{-a}^{a} q_1(x)\,\mathrm{d}x + \int_{-c}^{c} q_2(x)\,\mathrm{d}x = \mu F_N\left[1-\left(\frac{c}{a}\right)^2\right] \tag{25}$$

whence:

$$\frac{c}{a} = \sqrt{1 - \frac{F_T}{\mu F_N}} = \sqrt{1 - \widehat{F}_T} \tag{26}$$

From a comparison between Eqs. (17) and (24) we recognize that $q_1(x)$ and $q_2(x)$ for cylinders have the same dependence on x as the corresponding equations for spheres. Therefore, keeping F_N constant and steadily increasing F_T from zero, micro-slip immediately develops at the two edges of the contact area and spreads inwards according to Eq. (26). As F_T approaches μF_N, c tends to zero and the stick region shrinks to a line at $x = 0$. Any further attempt to increase F_T causes the contact to slide. It is also interesting to note that the applied tangential force can be decomposed into two parts, as previously shown for spheres and rough surfaces: the former supported by the contact domain in stick condition, F_T^{ST}, and the latter supported by the remaining part in slip condition, $F_T^{SL} = F_T - F_T^{ST}$. Again, the following results cannot be found elsewhere. Focusing our attention on the stick contribution, we have

$$F_T^{ST} = \int_{-c}^{c} q_1(x)\,\mathrm{d}x + \int_{-c}^{c} q_2(x)\,\mathrm{d}x = \\ = \frac{2}{\pi}\mu F_N \left\{ \frac{c}{a}\sqrt{1 - \left(\frac{c}{a}\right)^2} + \arctan\left[\frac{c}{a} \frac{1}{\sqrt{1 - \left(\frac{c}{a}\right)^2}} \right] \right\} - \mu F_N \left(\frac{c}{a}\right)^2 \tag{27}$$

which can also be expressed as a function of the applied tangential force using Eq. (26)

$$\widehat{F}_T^{ST} = \frac{2}{\pi} \left\{ \sqrt{\left(1 - \widehat{F}_T\right)\widehat{F}_T} + \arctan\left[\sqrt{\frac{1 - \widehat{F}_T}{\widehat{F}_T}} \right] \right\} + \widehat{F}_T - 1 \tag{28}$$

where also here the nondimensional variables $\widehat{F}_T$ and $\widehat{F}_T^{ST}$ have been suitably introduced.

Finally, it is possible to establish a relationship between the nondimensional contact area in stick condition, $\widehat{A}^{ST}$, and the nondimensional applied tangential force, $\widehat{F}_T$

$$\widehat{A}^{ST} = \frac{c}{a} = \sqrt{1 - \widehat{F}_T} \tag{29}$$

3.3 Smooth plane surfaces

Let us consider two half spaces in contact along their smooth ideal planes and compressed by a normal force, F_N. This problem corresponds to the limit case of contact between two ideal flat surfaces. When a tangential force $F_T < \mu F_N$ is subsequently applied at the interface level, all the points belonging to the planes remain in stick condition. On the other hand, when the tangential force reaches its critical value, i.e. $F_T = \mu F_N$, full-slip takes place instantaneously along the whole planes, since all the points in contact support the same normal pressure.

Under these limit conditions, the stick components of the tangential force and of the contact area are given by (in nondimensional form)

$$\widehat{F}_T^{ST} = \begin{cases} \widehat{F}_T, & 0 \le \widehat{F}_T < 1, \\ 0, & \widehat{F}_T = 1 \end{cases} \tag{30}$$

$$\widehat{A}^{ST} = \begin{cases} 1, & 0 \le \widehat{F}_T < 1, \\ 0, & \widehat{F}_T = 1 \end{cases} \tag{31}$$

A comparison between the obtained solutions for rough and smooth surfaces is proposed in Fig. 5. The nondimensional stick component of the tangential force vs. the total tangential force curves shown in Fig. 5a have a characteristic bell-shape. For a given value of the nondimensional applied tangential force, spheres show the lowest value of tangential force supported by the stick domain. Higher values are observed for cylinders and rough surfaces, whereas totally flat surfaces provide the limit situation corresponding to a straight line with a 45° slope, being $\widehat{F}_T^{ST} = \widehat{F}_T$ for $0 \le \widehat{F}_T < 1$ while for $\widehat{F}_T = 1$ a vertical drop takes place. It is interesting to note that the above order is maintained in the nondimensional stick contact area vs. nondimensional total tangential force diagram (see Fig. 5b). In this case, spheres have the lowest contact area in stick condition for a given applied tangential force with respect to cylinders and rough surfaces. The limit case of totally flat surfaces is now represented by a horizontal line corresponding to $\widehat{A}^{ST} = 1$ for $0 \le \widehat{F}_T < 1$, while for $\widehat{F}_T = 1$ once more a vertical drop takes place.

4 Modelling the problem of contact loss and related instabilities

In order to quantify the effect of contact loss on the tangential motion of rough surfaces, we propose an analytical model which extends the pioneering results obtained by Mindlin and Deresiewicz (1953) for smooth spheres. Due to the generality of the proposed methodology, this approach can also be applied to smooth

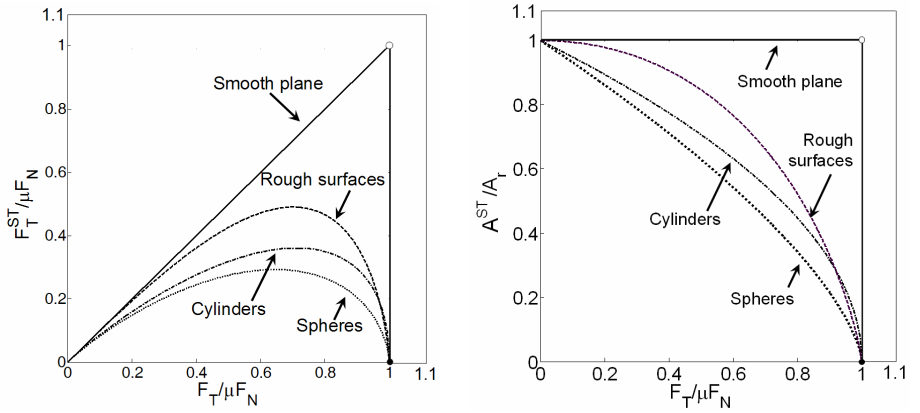

(a) Nondimensional stick tangential force (b) Nondimensional stick contact area

Figure 5: Nondimensional tangential force dependencies.

surfaces such as cylinders, spheres, or ideally flat surfaces, using the formulae derived in Section 3.

Regardless of the mechanism causing the contact loss, that may vary from a material to another, as discussed in the introduction, let us model this phenomenon as a loading condition consisting in a decreasing normal force followed by an increasing tangential force. When F_{N} is reduced by an amount ΔF_{N}, with the tangential load held constant, such a decrease would increase the separation, d, between the rough surfaces. Correspondingly, the real contact area is reduced from A_{r} to $A'_{\mathrm{r}} = A_{\mathrm{r}} - \Delta A_{\mathrm{r}}$ according to Eq. (13). However, the portions of the contact surface related to ΔA_{r} would no longer be in contact and would be unable to sustain tangential tractions. Consequently, before a reduction in normal load may by effected, it is necessary to remove the existing tangential tractions from this region. This removal can be accomplished by treating the i-th spherical asperity according to the formulation by Mindlin and Deresiewicz (1953). Hence, the reduction of the normal load causes a loss of contact in the annulus $a_i^{new} \leq r \leq a_i$. During the removal, the new contact area $r \leq a_i^{new}$ will be "frozen", i.e., no slip is permitted to take place in that region. Then, a distribution of tractions is added, so that the annulus $a_i^{new} \leq r \leq a_i$ becomes traction free. As demonstrated by Mindlin and Deresiewicz (1953), this leads to a resultant traction which will be in equilibrium with $(F'_{\mathrm{T}})_i = (F_{\mathrm{T}})_i - \mu\,(\Delta F_{\mathrm{N}})_i$. As regards the global behaviour of the rough surface, this will correspond to the summation of the individual behaviours of each asperities and therefore the resultant traction distribution will be in equilibrium with the new force $F'_{\mathrm{T}} = F_{\mathrm{T}} - \mu \Delta F_{\mathrm{N}}$.

This new equilibrium configuration would also be characterized by a relative tangential displacement g'_{T}, smaller than g_{T}, obtained by inverting Eq. (9). Now, holding the normal force constant at $F'_{\mathrm{N}} = F_{\mathrm{N}} - \Delta F_{\mathrm{N}}$, a subsequent increase in the tangential load would cause an increase in the relative tangential displacement and a progressive shrink of the stick part of the contact region.

As an illustrative example, let us consider the contact between a microscopically rough surface depicted in Fig. 2 with $\sigma^* = 2\ \mu$m, $\nu = 0.3$ and $\mu = 0.1$. Results are shown in Fig. 6.

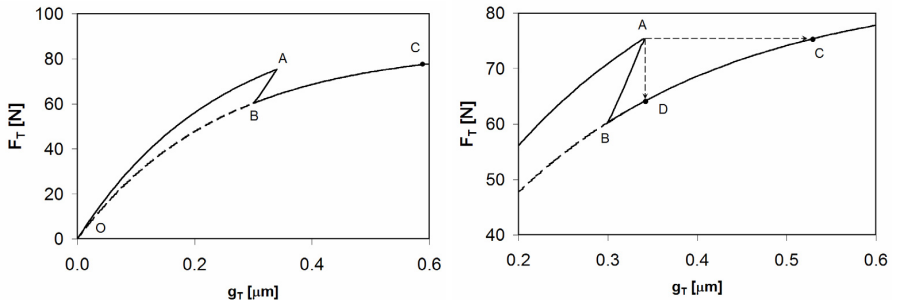

(a) Tangential load vs. relative tangential displacement diagram.

(b) Magnification of the previous diagram where snap-back (AD) and snap-through (AC) instabilities are shown.

Figure 6: Instabilities in the tangential load vs. sliding displacement diagram.

In this analysis, the normal load is kept constant at the value of 1 kN and the tangential displacement is progressively increased up to 0.34 μm, following the path OA in the tangential force vs. sliding displacement diagram. After reaching point A, the normal load is progressively reduced down to 0.85 kN and the equilibrium configurations corresponding to $F'_{\mathrm{T}} = F_{\mathrm{T}}^{\max} - \mu \Delta F_{\mathrm{N}}$ are progressively computed, step-by-step, for each value of ΔF_{N}. The mechanical response is thus represented by the nonlinear path AB, where each point corresponds to the solution of a problem obtained by imposing a reduced normal load $F'_{\mathrm{N}} = F_{\mathrm{N}} - \Delta F_{\mathrm{N}}$ and then applying an increasing tangential force rising from zero up to F'_{T} (see, e.g., the path OB). After point B, the tangential load is increased again, following the ascending branch BC.

Thus, a reduction in the normal load during tangential loading results into a jagged mechanical response of the system, with a branch AB with positive slope. This is a cause of mechanical instability, leading to energy release. In fact, if the driving parameter is the applied tangential load, then a subsequent increase in the tangential force F_{T} after point A may cause a *snap-through instability*, following the path

AC. The area of the region ABC is then released as a vibrational energy. Similarly, if the driving parameter is the sliding displacement, then a subsequent increase in g_T after point A will give rise to a vertical drop down to point D, with the occurrence of a *snap-back instability*. Also in this case, the area of the region ABD would be released as a vibrational energy. This suggests the possibility to apply the proposed theory to the analysis of the energy released in form of seismic waves during earthquakes, one of the most notable examples of stick-slip motion in civil engineering.

From the mechanical point of view, these results allows us to interpret the problem of stick-slip according to the Catastrophe Theory (Thom, 1975), in close analogy with the previous studies by Carpinteri (1985, 1989) on the snap-back instability of Mode I cohesive crack propagation in concrete members. Hence, the post-peak branch AB does not correspond to a simple elastic unloading and the phenomenon under consideration shares all the features typical of a cusp-catastrophe instability. In fact, in close analogy with the snap-back behavior of Mode I cohesive crack growth in plane concrete beams tested under three-point bending (Carpinteri, 1985, 1989), where the length of the crack may be used as the driving parameter to follow the unstable branch, the physical quantity which is a monotonically increasing function is herein represented by the total slipping contact area. On the other hand, the analogous of the beam deflection is now represented by the imposed sliding displacement at infinity, i.e., far from the interface. The total slipping contact area can be computed as the sum of the contact area in slip condition for the actual applied tangential force, plus the slipped real contact area due to the normal force reduction, ΔA_r. In nondimensional form we have

$$\widehat{A}^{\mathrm{SL}} = \frac{A^{\mathrm{SL}}}{A_r} = \left(1 - \widehat{A}^{\mathrm{ST}}\right) + \frac{\Delta A_r}{A_r} \tag{32}$$

where $\widehat{A}^{\mathrm{ST}}$ is given by Eq. (15) for rough surfaces with an exponential distribution of asperity heights (or by Eqs. (20), (29) and (31) for smooth surfaces), A_r is the initial real contact area before normal force reduction, and ΔA_r represents the amount of slipped contact area due to normal force reduction. Therefore, although the equilibrium conditions along the path AB correspond to lower tangential forces, *the total slipped contact area steadily increases*, giving rise to a *catastrophical response*. Using the total slipped contact area as the driving parameter, the virtual post-peak branch with positive slope in Fig. 6(a) can be captured (see the path AB in Fig. 7 which has now a negative slope), the obtained curve being now a single valued function of A_{SL}/A_r.

It is also interesting to note that the nonlinearity of the post-peak branch AB in Fig. 6(a) depends on the magnitude of the normal load reduction. For a reduction of

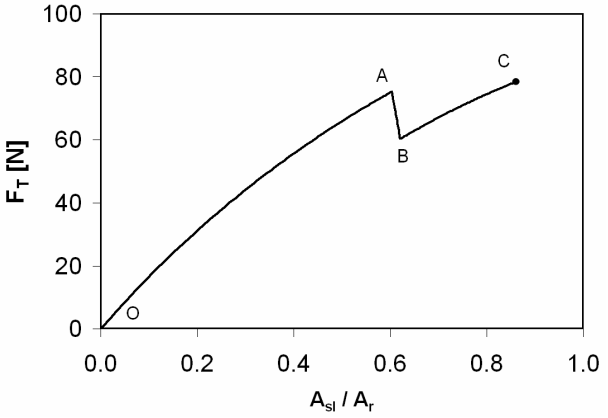

Figure 7: Tangential force vs. nondimensional total slipped contact area.

F_N from 1000 N to 800 N, the post-peak path is not far from a straight line (see Fig. 8), whereas its deviation from linearity is quite significant if further reductions are considered (see the different curves in Fig. 8, where the post-peak paths are depicted with dashed line).

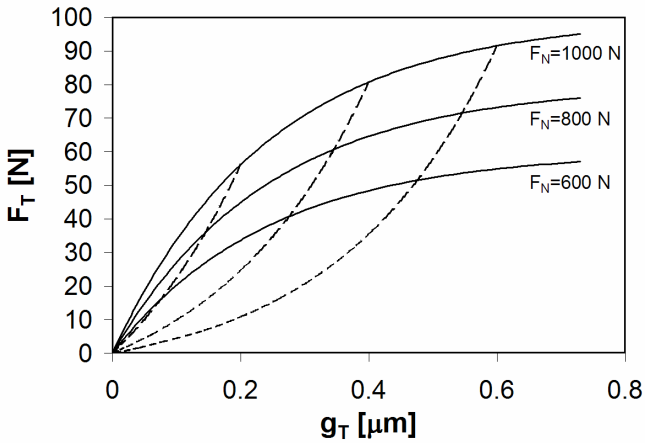

Figure 8: The nonlinearity of the post-peak paths.

Moreover, according to differential topology, a catastrophic behaviour of a mechanical system can be described by the properties of surfaces in many dimensions (manifolds). By definition, an elementary catastrophe is determined by its state

variable (the total slipped contact area in this case) and by one or more control variables. One of the elementary catastrophes is the cusp catastrophe (Thom, 1975). Here, the catastrophe manifold can be regarded as a three-dimensional response surface in the parameter space defined by the sliding displacement at infinity, the tangential force and the friction coefficient. This surface has a pleated shape and the edges of the pleat define the fold curve. For a given friction coefficient, the cross-section of the response surface provides a fold curve as those shown in Fig. 9. Note that the snap-back instability is even more severe when higher and higher friction coefficients are considered.

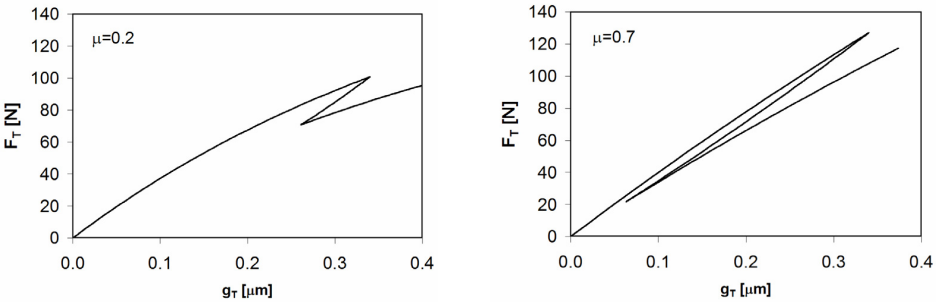

(a) Low friction coefficient. (b) High friction coefficient.

Figure 9: The effect of the friction coefficient on the mechanical response.

5 Conclusions

The problem of tangential contact between rough surfaces has been addressed. To this aim, a micromechanical model based on the Greenwood and Willamson contact model has been developed for the analysis of the tangential response of rough surfaces. Special attention has been given to the computation of the stick and slip components of the tangential force and the real contact area, obtaining useful and unprecedented closed-form solutions in the case of random rough surfaces with an exponential distribution of the asperity heights and of smooth surfaces, such as spheres, cylinders and ideal smooth planes.

Finally, according to the proposed theory, the problem of contact loss has been numerically simulated and it has been shown that this phenomenon leads to either snap-back or snap-through instabilities, depending on the adopted driving parameter of the contact problem. This demonstrates for the first time that the phenomenon of stick-slip may occur during the micro-slip motion of rough surfaces and manifests itself as a catastrophic instability, in close analogy with the problem of crack

propagation in cohesive solids. Hence, whenever a combination of the control variables (applied tangential force, sliding displacement, friction coefficient) crosses the bifurcation curve, a catastrophic change occurs and the control point jumps on the behaviour surface from the upper part of the pleat to the lower one. In this jump, the mechanical system completely changes its configuration. To follow the unstable branch, the driving parameter to be used is here represented by the nondimensional total slipped contact area. This state variable, which is an increasing monotonic function of time, has its analogous counterpart in the crack length for the problem of crack propagation in cohesive solids (Carpinteri, 1989).

Acknowledgement: The financial support provided by the European Union to the Leonardo da Vinci Project 2006-I/06/B/F/PP-154069 "Innovative Learning and Training on Fracture" (ILTOF), and the Program Vigoni 2007-2008 are gratefully acknowledged.

References

Borri-Brunetto, M., Chiaia, B., Paggi, M. (2006a): Multiscale models for contact mechanics of rough surfaces, Chapter 1 in: R. Buzio, U. Valbusa (Eds.), Advances in Contact Mechanics: Implications for Materials Science, Engineering & Biology, Research Signpost, Trivandrum (India), pp. 1-41, ISBN: 81-7895-221-1.

Borri-Brunetto, M., Carpinteri, A., Invernizzi, S., Paggi, M. (2006b): Microslip of rough surfaces under cyclic tangential loading, In: P. Wriggers, U. Nackenhorst (Eds.), *Analysis and Simulation of Contact Problems, Lecture Notes in Applied and Computational Mechanics*, vol. 27, pp. 333-340, Springer-Verlag, Berlin (Germany).

Bouissou, S., Petit, J.P., Barquins, M. (1998): Experimental evidence of contact loss during stick-slip: possible implications for seismic behaviours. *Tectonophysics*, vol. 295, pp. 341-350.

Brown, S.R., Scholz, C.H. (1985): Closure of random elastic surfaces in contact. *Journal of Geophysical Research*, vol. 90, pp. 5531-5545.

Bureau, L., Caroli, C., Baumberger, T. (2003): Elasticity and onset of frictional dissipation at a non-sliding multi-contact interface. *Proceedings of the Royal Society of London* Ser. A, vol. 459, pp. 2787-2805.

Carpinteri, A. (1985): Interpretation of the Griffith instability as a bifurcation of the global equilibrium. In *Application of Fract. Mech. to Cementitious Comp.* (Proc. NATO Adv. Res. Workshop, Evanston, USA, 1984), Ed. S.P. Shah, Martinus Nijhoff Publishers, Dordrecht, pp. 287-316.

Carpinteri, A. (1989): Cusp catastrophe interpretation of fracture instability. *Jour-*

nal of the Mechanics and Physics of Solids, vol. 37, pp. 567-582.

Carpinteri, A., Paggi, M. (2005): Size-scale effects on the friction coefficient. *International Journal of Solids and Structures*, vol. 42, pp. 2901-2910.

Carpinteri, A., Paggi, M. (2008): Size-scale effects on strength, friction and fracture energy of faults: a unified interpretation according to fractal geometry. *Rock Mechanics and Rock Engineering*, vol. 41, pp. 735-746.

Cattaneo, C. (1938): Sul contatto di due corpi elastici: distribuzione locale degli sforzi. *Rendiconti dell'Accademia Nazionale dei Lincei*, Serie 6, vol. 27, pp. 342-348, 434-436, 474-478.

Chen, C. Y.; Atkinson, C. (2009) The Stress Analysis of Thin Contact Layers: a Viscoelastic Case *CMES: Computer Modeling in Engineering & Sciences*, Vol. 48, No. 3, pp. 219-240

Ciavarella, M. (1998): The generalized Cattaneo partial slip plane contact problem. I-Theory, II-Examples. *International Journal of Solids and Structures*, vol. 35, pp. 2349-2378.

Ciavarella, M., Greenwood, J.A., Paggi, M. (2008): Inclusion of "interaction" in the Greenwood & Williamson contact theory. *Wear*, vol. 265, pp.729-734.

Comninou, M., Dundurs, J. (1978): Can two solids slide without slipping?. *International Journal of Solids and Structures*, vol. 14, pp. 251-260.

Desai, C.S., Drumm, E.C., Zaman, M.M. (1985): Cyclic testing and modeling of interfaces. *ASCE Journal of Geotechnical Engineering*, vol. 111, pp. 793-815.

Frémond, M., Isabella-Valenzi, P. (2006): Sthenic incompatibilityes in rigid bodies motion, In: P. Wriggers, U. Nackenhorst (Eds.), *Analysis and Simulation of Contact Problems, Lecture Notes in Applied and Computational Mechanics*, vol. 27, pp. 145–152, Springer-Verlag, Berlin (Germany).

Galli, M.; Oyen, M. L. (2009) Fast Identification of Poroelastic Parameters from Indentation Tests *CMES: Computer Modeling in Engineering & Sciences*, Vol. 48, No. 3, pp. 241-270

García-Aznar, J. M.; Pérez, M. A.; Moreo P. (2009) Modelling of Interfaces in Biomechanics and Mechanobiology *CMES: Computer Modeling in Engineering & Sciences*, Vol. 48, No. 3, pp. 271-302

Goodman, L.E., Brown, C.B. (1962): Energy dissipation in contact friction: constant normal load and cyclic tangential loading. *ASME Journal of Applied Mechanics*, vol. 84, pp. 17-22.

Greenwood, J.A., Williamson, J.B.P. (1966): The contact of nominally flat surfaces. *Proceedings of the Royal Society of London Ser. A*, vol. 295, pp. 300-319.

Guduru, P.R. (2007): Detachment of a rigid solid from an elastic wavy surface: Theory. *Journal of the Mechanics and Physics of Solids*, vol. 55, pp. 445-472.

Guduru, P.R., Bull, C. (2007): Detachment of a rigid solid from an elastic wavy surface: Experiments. *Journal of the Mechanics and Physics of Solids*, vol. 55, pp. 473-488.

Harnoy, A., Friedland, B., Rachoor, H. (1994): Modeling and simulation of elastic and friction forces in lubricated bearings for precise motion control. *Wear*, vol. 172, pp. 155-165.

Jäger, J. (1998): A new principle in contact mechanics, *ASME Journal of Tribology*, vol. 120, pp. 677-684.

Johnson, K.L. (1985): *Contact Mechanics*, Cambridge University Press, Cambridge.

Kikuchi, N., Oden, J.T. (1988): *Contact Problems in Elasticity: A study of Variational Inequalities and Finite Element Methods*. SIAM: Philadelphia, Ch. 13.

Kirsonava, V.N. (1967): The shear compliance of flat joints. *Machineering Tooling*, vol. 38, pp. 30-34.

Mindlin, R.D. (1949): Compliance of elastic bodies in contact. *ASME Journal of Applied Mechanics*, vol. 71, pp. 259-268.

Mindlin, R.D., Deresiewicz, H. (1953): Elastic spheres in contact under varying oblique force. *ASME Journal of Applied Mechanics*, vol. 20, pp. 327-344.

Nosonovsky, M., Bhushan, B. (2007): Multiscale friction mechanisms and hierarchical surfaces in nano- and bio-tribology. *Materials Science and Engineering R*, vol. 58, pp. 162-193.

Paggi, M., Zavarise, G., Carpinteri, A, (2007): Snap-back and snap-through instabilities due to contact loss in the stick-slip motion of rough surfaces. In: *Proceedings of the 18th AIMETA Congress of Theoretical and Applied Mechanics*, Brescia, Italy, on CD-ROM.

Persson, B.N.J. (2001): Elastic instabilities at a sliding interface. *Physical Review B*, vol. 63, 104101.

Putelat, T., Dawes, J.H.P., Willis, J.R. (2007): Sliding modes of two interacting frictional interfaces. *Journal of the Mechanics and Physics of Solids*, vol. 55, pp. 2073-2105.

Rooke, D.P., Edwards, P.R. (1988): Waveforms in fretting fatigue. *Fatigue and Fracture of Engineering Materials and Structures*, vol. 11, pp. 447-465.

Sainsot, P., Jacq, C., Nelias, D. (2002): A numerical model for elastoplastic rough contact. *CMES: Computer Modeling in Engineering & Sciences*, vol. 3 (4), pp.

497-506.

Willner, K. (2009) Constitutive Contact Laws in Structural Dynamics *CMES: Computer Modeling in Engineering & Sciences*, Vol. 48, No. 3, pp. 303-336

Song, Y., McFarland, D.M., Bergman, L.A., Vakakis, A.F. (2005): Stick-slip-slap interface response simulation: formulation and application of a general joint/interface element. *CMES: Computer Modeling in Engineering & Sciences*, vol. 10 (2), pp. 153-170.

Thom, R. (1975): *Structural Stability and Morphogenesis*, Benjamin, Reading, Massachusetts.

Yao, H., Gao, H. (2007): Multi-scale cohesive laws in hierarchical materials. *International Journal of Solids and Structures*, vol. 44, pp. 8177-8193.

Yoshizawa, H., Chen, Y.L., Israelachvili, J. (1993): Fundamental Mechanisms of Interfacial Friction I: Relation Between Adhesion and Friction. *Journal of Chemical Physics*, vol. 97, pp. 4128-4140.

Zavarise, G., Borri-Brunetto, M., Paggi, M. (2004): On the reliability of microscopical contact models. *Wear*, vol. 257, pp. 229-245.

Zavarise, G., Borri-Brunetto, M., Paggi, M. (2007): On the resolution dependence of micromechanical contact models. *Wear*, vol. 262, pp. 42-54.